Available online at www.sciencedirect.com
ScienceDirect
Journal of Computational Physics 226 (2007) 1968–1984
JOURNAL OF COMPUTATIONAL PHYSICS
www.elsevier.com/locate/jcp

Multi-symplectic Runge–Kutta–Nyström methods for nonlinear Schrödinger equations with variable coefficients

Jialin Hong [a,*,1], Xiao-yan Liu [a,b,2], Chun Li [a,c]

[a] State Key Laboratory of Scientific and Engineering Computing, Institute of Computational Mathematics and Scientific/Engineering Computing, Academy of Mathematics and Systems Science, Chinese Academy of Sciences, P.O. Box 2719, Beijing 100080, PR China
[b] Department of Mathematics, Northeast Normal University, Changchun 130024, PR China
[c] Graduate School of the Chinese Academy of Sciences, Beijing 100080, PR China

Received 30 November 2006; received in revised form 17 June 2007; accepted 22 June 2007
Available online 5 July 2007

Abstract

In this paper, we consider Runge–Kutta–Nyström (RKN) methods applied to nonlinear Schrödinger equations with variable coefficients (NLSEvc). Concatenating symplectic Nyström methods in spatial direction and symplectic Runge–Kutta methods in temporal direction for NLSEvc leads to multi-symplectic integrators, i.e. to numerical methods which preserve the multi-symplectic conservation law (MSCL), we present the corresponding discrete version of MSCL. It is shown that the multi-symplectic RKN methods preserve not only the global symplectic structure in time, but also local and global discrete charge conservation laws under periodic boundary conditions. We present a (4-order) multi-symplectic RKN method and use it in numerical simulation of quasi-periodically solitary waves for NLSEvc, and we compare the multi-symplectic RKN method with a non-multi-symplectic RKN method on the errors of numerical solutions, the numerical errors of discrete energy, discrete momentum and discrete charge. The precise conservation of discrete charge under the multi-symplectic RKN discretizations is attested numerically. Some numerical superiorities of the multi-symplectic RKN methods are revealed.

Keywords: Nonlinear Schrödinger equations; Multi-symplectic conservation law; Runge–Kutta–Nyström methods; Charge conservation law

1. Introduction

The nonlinear Schrödinger equation in its many versions is one of the most important models of mathematical physics, with applications to different fields such as plasma physics, nonlinear optics, water waves,

* Corresponding author.
E-mail address: hjl@lsec.cc.ac.cn (J. Hong).
[1] Supported by the Director Innovation Foundation of ICMSEC and AMSS, the Foundation of CAS, the NNSFC (No. 19971089 and No. 10371128) and the National Basic Research Program under the Grant 2005CB321701.
[2] Supported by China Postdoctoral Science Foundation and the Tianyuan Mathematics Funds of China (201546000) and the Funds of Northeast Normal University (11415000). The present address: School of Information, Renmin University of China, Beijing, PR China.

0021-9991/$ - see front matter © 2007 Elsevier Inc. All rights reserved.
doi:10.1016/j.jcp.2007.06.023

bimolecular dynamics and many other fields. And many numerical methods have been developed to solve it (see [5–7,9,13,14,19,21] and references therein). In the last two decades, symplectic methods have predominated over non-symplectic schemes for long-time numerical computations and nowadays applied to many fields of science which include celestial mechanics, quantum physics, statistics and so on [1,6,12,15,20]. The multi-symplectic integrators which preserve the discrete form of the multi-symplectic conservation law have been suggested in [3,19]. Some results on multi-symplectic methods have been presented in [1,3,7–11,13,14,16–19] and references therein. For Hamiltonian partial differential equations (PDEs) with constant coefficients, Reich in [19] considered Hamiltonian wave equations, and showed that the Gauss–Legendre discretization applied to the scalar wave equation (also to the nonlinear Schrödinger equation) both in temporal and spatial directions, leads to a multi-symplectic integrator (also see [10,13]), and some sufficient conditions for multi-symplecticity of partitioned Runge–Kutta (PRK) methods applied to Hamiltonian PDEs have been presented by Hong et al. [10], it has been shown that concatenating symplectic PRK methods in temporal and spatial directions leads to the multi-symplectic integrators, and some conservative properties on charge, energy and momentum for multi-symplectic Gauss–Legendre methods, multi-symplectic Runge–Kutta methods and multi-symplectic partitioned Runge–Kutta methods have been discussed in [10,11,13,14,17,19] and some references therein. Authors of [7–9] developed multi-symplectic methods, mainly centred box scheme, for some Hamiltonian PDEs with variable coefficients, including linear (nonlinear) Schrödinger equations and KdV equations, and related numerical analysis.

Now we pay attention to the special symplectic methods for special kinds of Hamiltonian ordinary differential equations. Nyström methods for the second order differential equation $\ddot{y} = g(y)$,

$$\begin{cases} l_i = g(y_0 + c_i h\dot{y}_0 + h^2 \sum_{j=1}^{s} a_{ij} l_j), \\ y_1 = y_0 + h\dot{y}_0 + h^2 \sum_{i=1}^{s} \beta_i l_i, \dot{y}_1 = \dot{y}_0 + h \sum_{i=1}^{s} b_i l_i, \end{cases}$$

are very useful and important in applications to some practical situations. In [22,23] (also see [6,20]), Suris obtained the symplectic conditions of Nyström methods as follows:

$$\begin{cases} \beta_i = b_i(1 - c_i) \quad \text{for } i = 1, \ldots, s, \\ b_i(\beta_j - a_{ij}) = b_j(\beta_i - a_{ji}) \quad \text{for } i, j = 1, \ldots, s, \end{cases}$$

which are very interesting, and guarantees the conservation of quadratic invariants ([6,15,20]).

In this paper, we consider nonlinear Schrödinger equations with variable coefficients (NLSEvc), which are proposed in [21] and have multi-symplectic conservation law and some physical conservative quantities ([7,9]). Because the derivative in NLSEvc in spatial direction is of second order, we apply symplectic Nyström methods in spatial direction and symplectic Runge–Kutta methods in temporal direction. Naturally, one wonders whether such concatenation methods lead to the multi-symplectic integrators, and whether they preserve classical conservation laws, such as the global symplecticity in time and the charge conservation laws and so on. In this paper, we show that such numerical methods preserve the multi-symplectic conservation law (so called multi-symplectic Runge–Kutta–Nyström (RKN) methods), and some important properties, such as the global symplecticity in time and the charge conservation law are also preserved. The charge conservation law can be seen as a quadratic invariant which is, in generical, not preserved by the symplectic integrators, even in the case of Hamiltonian ODEs ([6,15,20]). For the purpose of application, we proposed a (4-order) multi-symplectic RKN method and make use of it in the numerical simulation of quasi-periodically solitary waves of NLSEvc. In the numerical comparison with a (4-order) non multi-symplectic RKN method, we find out some superiorities of multi-symplectic RKN methods in numerical computation for NLSEvc.

This paper is organized as follows: In Section 2, we present the condition of multi-symplecticity of RKN methods. In order to study the classical conservative properties of multi-symplectic RKN methods, we discuss some local and global conservation laws, e.g., energy, momentum and charge, for NLSEvc. In Section 3, we show that the multi-symplectic RKN methods have the global symplectic conservation in time, and prove that they have the local discrete charge conservative property, thus have the global one which is very important in the application to some physical problems. In Section 4, in order to illustrate our theoretical results, we present a 4-order multi-symplectic RKN method and give some numerical experiments, especially, some numerical comparisons with a (4-order) non multi-symplectic RKN method. The conclusion of this paper is presented in Section 5.

2. Conservation laws

2.1. Multi-symplectic conservation law

We consider the following nonlinear Schrödinger equation with variable coefficients (NLSEvc)

$$\mathbf{i}\partial_t\psi + \alpha(t)\partial_{xx}\psi + \theta(t)V'(|\psi|^2)\psi = 0, \qquad (x,t) \in U \subset R^2, \tag{2.1}$$

where V, α and θ are smooth functions from R to R (for more details of (2.1), see [7,9,21]). Let $\psi = q + \mathrm{i}\, p$. Then (2.1) can be written in the form

$$\partial_t q = -\alpha(t)\partial_{xx}p - \theta(t)V'(q^2+p^2)p, \tag{2.2a}$$

$$\partial_t p = \alpha(t)\partial_{xx}q + \theta(t)V'(q^2+p^2)q. \tag{2.2b}$$

We introduce a pair of conjugate momenta $v = q_x$, $w = p_x$ and obtain a Hamiltonian PDE

$$M\partial_t z + K\partial_x z = \nabla_z S(z,t), \tag{2.3}$$

where $z = (q,p,v,w)^{\mathrm{T}}$, M and K are skew-symmetric matrices,

$$M = \begin{pmatrix} 0 & -1 & 0 & 0 \\ 1 & 0 & 0 & 0 \\ 0 & 0 & 0 & 0 \\ 0 & 0 & 0 & 0 \end{pmatrix}, \quad K = \alpha(t)\begin{pmatrix} 0 & 0 & 1 & 0 \\ 0 & 0 & 0 & 1 \\ -1 & 0 & 0 & 0 \\ 0 & -1 & 0 & 0 \end{pmatrix},$$

and the smooth function $S(z,t) = -\frac{1}{2}\theta(t)V(q^2+p^2) - \frac{1}{2}\alpha(t)(v^2+w^2)$. Eq. (2.3) has a multi-symplectic conservation law (see [2,3,7,9,13–15])

$$\frac{\partial\omega}{\partial t} + \frac{\partial\kappa}{\partial x} = 0, \tag{2.4}$$

where ω and κ are pre-symplectic forms,

$$\omega = \frac{1}{2}\mathrm{d}z \wedge M\,\mathrm{d}z \qquad \text{and} \qquad \kappa = \frac{1}{2}\mathrm{d}z \wedge K\,\mathrm{d}z. \tag{2.5}$$

The corresponding equations for the differential one forms $\mathrm{d}a = (\mathrm{d}q, \mathrm{d}p, \mathrm{d}v, \mathrm{d}w)^T$ are given by

$$\partial_t\,\mathrm{d}q + \alpha(t)\partial_x\,\mathrm{d}w = -\theta(t)[V'(q^2+p^2)\,\mathrm{d}p + (2pq\,\mathrm{d}q + 2p^2\,\mathrm{d}p)V''(q^2+p^2)], \tag{2.6a}$$

$$-\partial_t\,\mathrm{d}p + \alpha(t)\partial_x\,\mathrm{d}v = -\theta(t)[V'(q^2+p^2)\,\mathrm{d}q + (2pq\,\mathrm{d}p + 2q^2\,\mathrm{d}q)V''(q^2+p^2)], \tag{2.6b}$$

$$\partial_x\,\mathrm{d}q = \mathrm{d}v, \tag{2.6c}$$

$$\partial_x\,\mathrm{d}p = \mathrm{d}w, \tag{2.6d}$$

where we use the fact that the exterior derivative operator d can commute with the partial derivative operators ∂_t or ∂_x. From (2.6a), (2.6b) it follows that

$$\partial_t\,\mathrm{d}q \wedge \mathrm{d}p + \alpha(t)\partial_x\,\mathrm{d}w \wedge \mathrm{d}p = -2\theta(t)qpV''(q^2+p^2)dq \wedge dp, \tag{2.7a}$$

$$-\partial_t\,\mathrm{d}p \wedge \mathrm{d}q + \alpha(t)\partial_x\,\mathrm{d}v \wedge \mathrm{d}q = -2\theta(t)qpV''(q^2+p^2)\,\mathrm{d}p \wedge \mathrm{d}q. \tag{2.7b}$$

This leads the multi-symplectic conservation law(MSCL)

$$\partial_t(\mathrm{d}p \wedge \mathrm{d}q) + \alpha(t)\partial_x(\mathrm{d}q \wedge \mathrm{d}v + \mathrm{d}p \wedge \mathrm{d}w) = 0. \tag{2.8}$$

Now we rewrite (2.3) as the following form

$$-\alpha(t)\partial_x v = -\partial_t p + \theta(t)V'(q^2+p^2)q, \tag{2.9a}$$

$$-\alpha(t)\partial_x w = \partial_t q + \theta(t)V'(q^2+p^2)p, \tag{2.9b}$$

$$\partial_x q = v, \tag{2.9c}$$

$$\partial_x p = w. \tag{2.9d}$$

Now let us consider the multi-symplecticity of concatenating Nyström methods in spatial direction and Runge–Kutta methods in temporal direction for NLSEvc (2.1). In order to process the numerical discretizaiton, we introduce a uniform grid [12] $(x_j, t_k) \in R^2$ with mesh-length Δt in the t-direction and mesh-length Δx in the x-direction, and denote the value of the function $\psi(x,t)$ at the mesh point (x_j, t_k) by ψ_j^k. For (2.9a)–(2.9d), in x-direction applying an s-stage Nyström method, with coefficients $\{a_{m,j}\}, \{b_m\}, \{\beta_m\}$ and $\{c_m\}$, and in t-direction applying an r-stage Runge–Kutta method with coefficients $\{\tilde{a}_{k,i}\}, \{\tilde{b}_k\}$ and $\tilde{d}_k = \sum_{j=1}^{s} \tilde{a}_{kj}$, it is concluded that

$$Q_{l,m}^k = q_l^k + c_m \Delta x v_l^k + \Delta x^2 \sum_{j=1}^{s} a_{mj} \partial_{xx} Q_{l,j}^k, \tag{2.10a}$$

$$P_{l,m}^k = p_l^k + c_m \Delta x w_l^k + \Delta x^2 \sum_{j=1}^{s} a_{mj} \partial_{xx} P_{l,j}^k, \tag{2.10b}$$

$$v_{l+1}^k = v_l^k + \Delta x \sum_{m=1}^{s} b_m \partial_{xx} Q_{l,m}^k, \tag{2.10c}$$

$$w_{l+1}^k = w_l^k + \Delta x \sum_{m=1}^{s} b_m \partial_{xx} P_{l,m}^k, \tag{2.10d}$$

$$q_{l+1}^k = q_l^k + \Delta x v_l^k + \Delta x^2 \sum_{m=1}^{s} \beta_m \partial_{xx} Q_{l,m}^k, \tag{2.10e}$$

$$p_{l+1}^k = p_l^k + \Delta x w_l^k + \Delta x^2 \sum_{m=1}^{s} \beta_m \partial_{xx} P_{l,m}^k, \tag{2.10f}$$

$$Q_{l,m}^k = q_{l,m}^0 + \Delta t \sum_{i=1}^{r} \tilde{a}_{ki} \partial_t Q_{l,m}^i, \tag{2.10g}$$

$$P_{l,m}^k = p_{l,m}^0 + \Delta t \sum_{i=1}^{r} \tilde{a}_{ki} \partial_t P_{l,m}^i, \tag{2.10h}$$

$$q_{l,m}^1 = q_{l,m}^0 + \Delta t \sum_{k=1}^{r} \tilde{b}_k \partial_t Q_{l,m}^k, \tag{2.10i}$$

$$p_{l,m}^1 = p_{l,m}^0 + \Delta t \sum_{k=1}^{r} \tilde{b}_k \partial_t P_{l,m}^k, \tag{2.10j}$$

$$\partial_t Q_{l,m}^k = -\alpha^k \partial_{xx} P_{l,m}^k - \theta^k V'(Q_{l,m}^k)^2 + (P_{l,m}^k)^2 P_{l,m}^k, \tag{2.10k}$$

$$\partial_t P_{l,m}^k = \alpha^k \partial_{xx} Q_{l,m}^k + \theta^k V'(Q_{l,m}^k)^2 + (P_{l,m}^k)^2 Q_{l,m}^k. \tag{2.10l}$$

The notations above are in the following sense, $Q_{l,m}^k \approx q((l+c_m)\Delta x, \tilde{d}_k \Delta t), q_l^k \approx q(l\Delta x, \tilde{d}_k \Delta t)$, $\partial_t Q_{l,m}^k \approx \partial_t q((l+c_m)\Delta x, \tilde{d}_k \Delta t)$, $\partial_{xx} Q_{l,m}^k \approx \partial_{xx} q((l+c_m)\Delta x, \tilde{d}_k \Delta t)$, $P_{l,m}^k \approx p((l+c_m)\Delta x, \tilde{d}_k \Delta t)$, $p_l^k \approx p\ (l\Delta x, \tilde{d}_k \Delta t)$, $\partial_t P_{l,m}^k \approx \partial_t p((l+c_m)\Delta x, \tilde{d}_k \Delta t)$, $\partial_{xx} P_{l,m}^k \approx \partial_{xx} p((l+c_m)\Delta x, \tilde{d}_k \Delta t)$, $v_l^k \approx v(l\Delta x, \tilde{d}_k \Delta t)$, $\alpha^k = \alpha(\tilde{d}_k \Delta t), \theta^k = \theta(\tilde{d}_k \Delta t)$, $p_{l,m}^0 \approx p((l+c_m)\Delta x, 0)$, $q_{l,m}^0 \approx q((l+c_m)\Delta x, 0)$, $p_{l,m}^1 \approx p((l+c_m)\Delta x, \Delta t)$, $q_{l,m}^1 \approx q((l+c_m)\Delta x, \Delta t)$, and so on.

The following result is the characterization of multi-symplectic RKN methods for NLSEvc, it has a similar proof (therefore omitted) to the results in [10,14,19].

Theorem 1. *In the method (2.10a)–(2.10l), if*

$$\beta_m = b_m(1 - c_m),\ b_m(\beta_j - a_{mj}) = b_j(\beta_m - a_{jm}), \quad \text{for } m, j = 1, 2, \ldots, s, \tag{2.11}$$

and

$$\tilde{b}_k \tilde{b}_i = \tilde{b}_k \tilde{a}_{ki} + \tilde{b}_i \tilde{a}_{ik}, \qquad \text{for } i, k = 1, 2, \ldots, r, \tag{2.12}$$

then the method (2.10a)–(2.10l) is multi-symplectic with the discrete multi-symplectic conservation law

$$\begin{aligned}&\Delta x\sum_{m=1}^{s} b_m(dq_{l,m}^1\wedge dp_{l,m}^1 - dq_{l,m}^0\wedge dp_{l,m}^0)\\&-\Delta t\sum_{k=1}^{r}\tilde{b}_k\alpha^k(dq_{l+1}^k\wedge dv_{l+1}^k - dq_l^k\wedge dv_l^k + dp_{l+1}^k\wedge dw_{l+1}^k - dp_l^k\wedge dw_l^k)=0.\end{aligned}\tag{2.13}$$

2.2. Some important classical conservation laws and their discretizations

As a preparation of the further discussion, we present some classical conservation laws. For the Hamiltonian PDE (2.3), it has a local momentum conservation law (MCL)

$$\frac{\partial I}{\partial t}+\frac{\partial G}{\partial x}=0\tag{2.14}$$

with momentum density $I=\frac{1}{2}z^{\mathrm{T}}Mz_x$ and momentum flux $G=S(z)-\frac{1}{2}z^{\mathrm{T}}Mz_t$. Evidently, we can rewrite $I(z)$ and $G(z)$ as the following compact forms

$$I(z)=\frac{1}{2}\Im(\overline{\partial_x\psi}\psi)\quad\text{and}\quad G(z)=-\frac{1}{2}\Im(\overline{\partial_t\psi}\psi)-\frac{\alpha(t)}{2}|\partial_x\psi|^2-\frac{\theta(t)}{2}V(|\psi|^2),$$

where $\Im$ denotes the imaginary part of complex number.

Now we take a product with (2.3) by $(Mz)^{\mathrm{T}}$ and notice that $(Mz)^{\mathrm{T}}\nabla_z S(z)$ vanishes, it follows that $(Mz)^{\mathrm{T}}Mz_t+(Mz)^{\mathrm{T}}Kz_x=0$. Since $z_x^{\mathrm{T}}M^{\mathrm{T}}Kz=0$, the above equation can be written as

$$\partial_t((Mz)^{\mathrm{T}}Mz)+\partial_x(2z^{\mathrm{T}}M^{\mathrm{T}}Kz)=0.\tag{2.15}$$

It is equivalent to a compact form

$$\partial_t(|\psi|^2)+\partial_x(\mathbf{i}\overline{\psi}\partial_x\psi-\mathbf{i}\psi\overline{\partial_x\psi})=0,$$

which is the local charge conservation law. The above two local conservation laws (2.14) and (2.15) can lead to the global properties of the system under appropriate assumptions (e.g., suitable boundary conditions).

Throughout this context, we assume that the solution is smooth enough, the spatial interval we consider is $[x_L,x_R]$. If $\psi(x,t)$ and $\partial_x\psi(x,t)$ satisfy periodic boundary conditions $\psi(x_L,t)=\psi(x_R,t)$ and $\partial_x\psi(x_L,t)=\partial_x\psi(x_R,t)$, respectively (here requires that $\psi(x_L,t)$ and $\partial_x\psi(x_L,t)$ are finite), for any t where is defined, then we will have two global conservation laws corresponding to the above two local ones, respectively,

$$\frac{\mathrm{d}}{\mathrm{d}t}\mathcal{I}(z)(t)=0\tag{2.16}$$

and

$$\frac{\mathrm{d}}{\mathrm{d}t}\mathcal{C}(z)(t)=0,\tag{2.17}$$

where $\mathcal{I}(z)(t)\triangleq\int_{x_L}^{x_R}I(z(x,t))\,\mathrm{d}x$ is the total momentum and $\mathcal{C}(z)(t)\triangleq\int_{x_L}^{x_R}|\psi(x,t)|^2\,\mathrm{d}x$ is the charge, which is also called mass or plasmon number (or wave power) in different scientific fields. For simplicity, we omit the proofs of the global conservation laws here.

Now we take $\tau=\Delta t$ and $h=\Delta x$, we integrate the local momentum conservation law (2.14) over the local domain $[0,\ \tau]\times[0,h]$, namely

$$\int_0^h[I(z(x,\tau))-I(z(x,0))]\mathrm{d}x+\int_0^\tau[G(z(h,t))-G(z(0,t))]\,\mathrm{d}t=0.\tag{2.18}$$

Corresponding to the discretization (2.10), we use a discrete form

$$M_{le}\triangleq h\sum_{m=1}^{s}b_m(I(z_m^1)-I(z_m^0))+\tau\sum_{k=1}^{r}\tilde{b}_k(G(z_1^k)-G(z_0^k))\tag{2.19}$$

to approximate the left side of (2.18). Similarly, it follows from (2.15) that

$$\int_0^h [C(z(x,\tau)) - C(z(x,0))]\,\mathrm{d}x + \int_0^\tau [J(z(h,t)) - J(z(0,t))]\,\mathrm{d}t = 0, \tag{2.20}$$

where $C(z) = (Mz)^{\mathrm{T}}Mz$ and $J(z) = 2z^{\mathrm{T}}M^{\mathrm{T}}Kz$ are the charge density and the charge flow, respectively. Thus, we define

$$C_{le} \triangleq h \sum_{m=1}^{s} b_m (C(z_m^1) - C(z_m^0)) + \tau \sum_{k=1}^{r} \tilde{b}_k (J(z_1^k) - J(z_0^k)) \tag{2.21}$$

as the discrete form of the left side of (2.20). In order to investigate the global conservation laws in the subsequent numerical simulations, we give the approximations for them. The discrete momentum and the discrete charge at the time t_n are defined by

$$\mathcal{I}_d(n) = \frac{h}{2} \sum_{l=0}^{N-1} \sum_{m=1}^{s} b_m \Im(\overline{\phi_{l,m}^n} \psi_{l,m}^n), \tag{2.22}$$

and

$$\mathcal{C}_d(n) = h \sum_{l=0}^{N-1} \sum_{m=1}^{s} b_m |\psi_{l,m}^n|^2 \tag{2.23}$$

respectively.

For a general Hamiltonian PDE of the abstract form (2.3), if the two skew symmetric matrices M and K are independent of t and the multi-symplectic Hamiltonian $S(z,t)$ does not depend on t explicitly, namely, if $\alpha(t) = \text{constant}$ and $\theta(t) = \text{constant}$, we will obtain the local energy conservation law

$$\frac{\partial E}{\partial t} + \frac{\partial F}{\partial x} = 0 \tag{2.24}$$

with energy density $E = S(z) - \frac{1}{2} z^{\mathrm{T}} K z_x$ and energy flux $F = \frac{1}{2} z^{\mathrm{T}} K z_t$, and the global energy conservation law

$$\frac{\mathrm{d}}{\mathrm{d}t} \mathcal{E}(z)(t) = 0 \tag{2.25}$$

provided with the periodic boundary conditions listed above, where $\mathcal{E}(z)(t) \triangleq \int_{x_L}^{x_R} E(z(x,t))\,\mathrm{d}x$. As to the NLSEvc in this context, however, the two quantities are not conserved. The discrete local energy variation is defined by

$$E_{le} \triangleq h \sum_{m=1}^{s} b_m (E(z_m^1) - E(z_m^0)) + \tau \sum_{k=1}^{r} \tilde{b}_k (F(z_1^k) - F(z_0^k)), \tag{2.26}$$

and the discrete total energy at t_n is defined by

$$\mathcal{E}_d(n) = h \sum_{l=0}^{N-1} \sum_{m=1}^{s} b_m \left(-\frac{\alpha(t_n)}{2} \Re(\overline{\psi_{l,m}^n} \partial_x \phi_{l,m}^n) - \frac{\theta(t_n)}{2} V(|\psi_{l,m}^n|^2) \right). \tag{2.27}$$

3. Total symplecticity and discrete charge conservation law

By using the complex-valued state variable $z = (\psi, \phi)^{\mathrm{T}} \in C^2, \partial_x \psi = \phi$, we can rewrite the multi-symplectic formulation of NLSEvc in the following equivalent compact form

$$\mathbf{i}\partial_t \psi + \alpha(t)\partial_x \phi = -\theta(t) V'(|\psi|^2)\psi,$$
$$\partial_x \psi = \phi.$$

Now we make use of the symplectic Nyström method in x-direction and the symplectic Runge–Kutta method in t-direction, a multi-symplectic method reads

$$\Psi_{l,m}^k = \psi_l^k + c_m \Delta x \phi_l^k + \Delta x^2 \sum_{j=1}^{s} a_{mj} \partial_{xx} \Psi_{l,j}^k, \tag{3.1a}$$

$$\phi_{l+1}^k = \phi_l^k + \Delta x \sum_{m=1}^{s} b_m \partial_{xx} \Psi_{l,m}^k, \tag{3.1b}$$

$$\psi_{l+1}^k = \psi_l^k + \Delta x \phi_l^k + \Delta x^2 \sum_{m=1}^{s} \beta_m \partial_{xx} \Psi_{l,m}^k, \tag{3.1c}$$

$$\Psi_{l,m}^k = \psi_{l,m}^0 + \Delta t \sum_{i=1}^{r} \tilde{a}_{ki} \partial_t \Psi_{l,m}^i, \tag{3.1d}$$

$$\psi_{l,m}^1 = \psi_{l,m}^0 + \Delta t \sum_{k=1}^{r} \tilde{b}_k \partial_t \Psi_{l,m}^k, \tag{3.1e}$$

$$\mathbf{i}\partial_t \Psi_{l,m}^k = -\alpha^k \partial_{xx} \Psi_{l,m}^k - \theta^k V'(|\Psi_{l,m}^k|^2) \Psi_{l,m}^k. \tag{3.1f}$$

The discrete conservation of multi-symplecticity as discussed in §2 is a local property of the Hamiltonian PDEs. The global symplecticity in time and the charge are the important conservation quantities for NLSEvc (2.1), and the charge conservation law plays an important role in self-focusing of laser in dielectrics, propagation of signals in optical fibers, 1D Heisenberg magnets and so on.

An important question is if the multi-symplectic RKN methods preserve the discrete global symplecticity in time and the discrete charge under the appropriate boundary conditions.

To answer this question, firstly we aim to obtain the discrete global symplecticity conservation. Use the same technique as in [10,11] under the periodic boundary conditions we integrate the multi-symplectic conservation law (2.4) over the spatial interval $[-L, L]$, which yields the following identity

$$0 = \int_{-L}^{L} \left(\frac{\partial}{\partial t} \omega + \frac{\partial}{\partial x} \kappa \right) \mathrm{d}x = \frac{\mathrm{d}}{\mathrm{d}t} \int_{-L}^{L} \omega \, \mathrm{d}x,$$

namely,

$$\int_{-L}^{L} \omega(x,t) \, \mathrm{d}x = \int_{-L}^{L} \omega(x,0) \, \mathrm{d}x, \tag{3.2}$$

which shows the global symplecticity is conserved in time in the continuous case. By summing the discrete symplectic conservation law over all spatial grid points, we have

$$0 = h \sum_{l=0}^{N-1} \sum_{m=1}^{s} b_m (\omega_{l,m}^1 - \omega_{l,m}^0) + \tau \sum_{l=0}^{N-1} \sum_{k=1}^{r} \tilde{b}_k (\kappa_{l+1,0}^k - \kappa_{l,0}^k) = h \sum_{l=0}^{N-1} \sum_{m=1}^{s} b_m (\omega_{l,m}^1 - \omega_{l,m}^0),$$

where the last equality comes from the periodic boundary condition (or zero boundary condition) on the spatial domain. This implies the following discrete total symplectic conservation law in time

$$h \sum_{l=0}^{N-1} \sum_{m=1}^{s} b_m \omega_{l,m}^1 = h \sum_{l=0}^{N-1} \sum_{m=1}^{s} b_m \omega_{l,m}^0. \tag{3.3}$$

Comparing (3.2) with (3.3), we find that (3.3) is the discrete approximation of (3.2) and we conclude that under appropriate boundary conditions, the multi-symplectic RKN methods have the discrete global symplectic conservation law in time, that is, the local symplectic property implies the global one.

Now we show that the discrete (local and global) charge conservation laws are preserved by means of the multi-symplectic RKN methods for NLSEvc with appropriate boundary conditions.

Theorem 2. *In the method* (3.1a)–(3.1f), *assume that*

$$\beta_m = b_m(1 - c_m), \ b_m(\beta_j - a_{mj}) = b_j(\beta_m - a_{jm}), \ \textit{for } m, j = 1, 2, \ldots, s,$$

and

$$\tilde{b}_k \tilde{b}_i = \tilde{b}_k \tilde{a}_{ki} + \tilde{b}_i \tilde{a}_{ik}, \quad \textit{for } i, k = 1, 2, \ldots, r,$$

then the discretization (3.1) *has a discrete local charge conservation law*

$$h\sum_{m=1}^{s} b_m(|\psi_{l,m}^1|^2 - |\psi_{l,m}^0|^2) + \mathbf{i}\tau\sum_{k=1}^{r}\tilde{b}_k\alpha^k[(\psi_{l+1}^k\overline{\phi_{l+1}^k} - \phi_{l+1}^k\overline{\psi_{l+1}^k}) - (\psi_l^k\overline{\phi_l^k} - \phi_l^k\overline{\psi_l^k})] = 0. \tag{3.4}$$

Proof 1. (3.1a)–(3.1f) imply

$$\begin{aligned}|\psi_{l,m}^1|^2 - |\psi_{l,m}^0|^2 &= \overline{\psi_{l,m}^1}\psi_{l,m}^1 - \overline{\psi_{l,m}^0}\psi_{l,m}^0 \\ &= \tau\sum_{k=1}^{r}\tilde{b}_k(\overline{\Psi_{l,m}^k}\partial_t\Psi_{l,m}^k + \overline{\partial_t\Psi_{l,m}^k}\Psi_{l,m}^k) + \tau^2\sum_{i,k=1}^{r}(\tilde{b}_k\tilde{b}_i - \tilde{b}_k\tilde{a}_{ki} - \tilde{b}_i\tilde{a}_{ik})\overline{\partial_t\Psi_{l,m}^k}\partial_t\Psi_{l,m}^i.\end{aligned}$$

By making use of $\tilde{b}_k\tilde{b}_i = \tilde{b}_k\tilde{a}_{ki} + \tilde{b}_i\tilde{a}_{ik}$, we have

$$\sum_{m=1}^{s} b_m(|\psi_{l,m}^1|^2 - |\psi_{l,m}^0|^2) = \tau\sum_{k=1}^{r}\tilde{b}_k\sum_{m=1}^{s} b_m(\overline{\Psi_{l,m}^k}\partial_t\Psi_{l,m}^k + \overline{\partial_t\Psi_{l,m}^k}\Psi_{l,m}^k). \quad \square \tag{3.5}$$

On the other hand, it follows that

$$\begin{aligned}\overline{\psi_{l+1}^k}\phi_{l+1}^k - \overline{\psi_l^k}\phi_l^k &= h\overline{\phi_l^k}\phi_l^k + h\sum_{m=1}^{s} b_m\overline{\Psi_{l,m}^k}\partial_{xx}\Psi_{l,m}^k + h^2\sum_{m=1}^{s}\beta_m\overline{\partial_{xx}\Psi_{l,m}^k}\phi_l^k + h^2\sum_{m=1}^{s} b_m(1-c_m)\overline{\phi_l^k}\partial_{xx}\Psi_{l,m}^k \\ &\quad + h^3\sum_{m,j=1}^{s} b_m(\beta_j - a_{mj})\overline{\partial_{xx}\Psi_{l,j}^k}\partial_{xx}\Psi_{l,m}^k.\end{aligned}$$

By using $\beta_m = b_m(1-c_m)$, we have

$$\overline{\psi_{l+1}^k}\phi_{l+1}^k - \overline{\psi_l^k}\phi_l^k = h|\phi_l^k|^2 + h\sum_{m=1}^{s} b_m\overline{\Psi_{l,m}^k}\partial_{xx}\Psi_{l,m}^k + 2h^2\sum_{m=1}^{s}\beta_m\Re(\overline{\partial_{xx}\Psi_{l,m}^k}\phi_l^k) + h^3\sum_{m,j=1}^{s} b_m(\beta_j - a_{mj})\overline{\partial_{xx}\Psi_{l,j}^k}\partial_{xx}\Psi_{l,m}^k, \tag{3.6}$$

where $\Re(u)$ denotes the real part of the complex u.

Secondly, we can get

$$\begin{aligned}\psi_{l+1}^k\overline{\phi_{l+1}^k} - \psi_l^k\overline{\phi_l^k} &= \overline{\overline{\psi_{l+1}^k}\phi_{l+1}^k - \overline{\psi_l^k}\phi_l^k} = h|\phi_l^k|^2 + h\sum_{m=1}^{s} b_m\Psi_{l,m}^k\overline{\partial_{xx}\Psi_{l,m}^k} + 2h^2\sum_{m=1}^{s}\beta_m\Re(\overline{\partial_{xx}\Psi_{l,m}^k}\phi_l^k) \\ &\quad + h^3\sum_{m,j=1}^{s} b_j(\beta_m - a_{jm})\overline{\partial_{xx}\Psi_{l,j}^k}\partial_{xx}\Psi_{l,m}^k.\end{aligned} \tag{3.7}$$

Subtracting (3.7) from (3.6) and using the condition $b_j(\beta_m - a_{jm}) = b_m(\beta_j - a_{mj})$, we obtain

$$(\overline{\psi_{l+1}^k}\phi_{l+1}^k - \overline{\psi_l^k}\phi_l^k) - (\overline{\phi_{l+1}^k}\psi_{l+1}^k - \overline{\phi_l^k}\psi_l^k) = h\sum_{m=1}^{s} b_m(\overline{\Psi_{l,m}^k}\partial_{xx}\Psi_{l,m}^k - \partial_{xx}\overline{\Psi_{l,m}^k}\Psi_{l,m}^k). \tag{3.8}$$

It follows from (3.1f) that

$$\overline{\Psi_{l,m}^k}\partial_t\Psi_{l,m}^k + \overline{\partial_t\Psi_{l,m}^k}\Psi_{l,m}^k = \mathbf{i}\alpha^k(\overline{\Psi_{l,m}^k}\partial_{xx}\Psi_{l,m}^k - \overline{\partial_{xx}\Psi_{l,m}^k}\Psi_{l,m}^k). \tag{3.9}$$

Combining (3.5), (3.8) and (3.9), we complete the proof.

From the above theorem, we obtain the preservation of the global charge conservation law of multi-symplectic RKN methods as follows.

Theorem 3. *Under the assumptions of Theorem 2, if the periodic boundary condition or zero boundary conditions hold for (2.1), i.e.* $\psi_N^n = \psi_0^{n,k}, \partial_x\psi_N^{n,k} = \partial_x\psi_0^{n,k}$, *or* $\psi_N^{n,k} = \psi_0^{n,k} = 0$, *then the method (3.1) satisfies the discrete charge conservation law, that is,*

$$h\sum_{l=0}^{N-1}\sum_{m=1}^{s} b_m|\psi_{l,m}^n|^2 = \textit{constant},$$

where $\psi^n_{l,m} \approx \psi((l+c_m)h, n\tau), \psi^{n,k}_{l,m} \approx \psi((l+c_m)h, (n+\tilde{d}_k)\tau)$ *and so on. When* $n = 0$ *we always omit the subscript* n *for simplicity, and* n *is a nonnegative integer here.*

Proof 2. Due to Theorem 2, taking the sum of the equation (3.4) over the spatial grid points, it follows that

$$h\sum_{l=0}^{N-1}\sum_{m=1}^{s} b_m(|\psi^1_{l,m}|^2 - |\psi^0_{l,m}|^2) = -\mathbf{i}\tau\sum_{k=1}^{r}\tilde{b}_k\alpha^k[(\overline{\psi^k_N}\phi^k_N - \overline{\psi^k_0}\phi^k_0) - (\overline{\phi^k_N}\psi^k_N - \overline{\phi^k_0}\psi^k_0)].$$

If the boundary conditions satisfy $\psi^k_N = \psi^k_0, \phi^k_N = \phi^k_0$, or $\psi^k_N = \psi^k_0 = 0$, then

$$h\sum_{l=0}^{N-1}\sum_{m=1}^{s} b_m(|\psi^1_{l,m}|^2 - |\psi^0_{l,m}|^2) = 0,$$

this completes the proof. □

Theorems 2 and 3 are non-trivial extensions of results on the quadratic invariants of symplectic RKN methods for Hamiltonian ODEs to the multi-symplectic RKN methods for NLSEvc. In numerical experiments in the next section, in fact, the charge conservation law of NLSEvc will be preserved precisely, in the round-off errors of computer, by means of the multi-symplectic RKN methods.

4. Numerical experiments

The numerical experiments of 2-order multi-symplectic RKN schemes (the Goldberg scheme and its generalization) can be found in [9]. In this section, we present a 4-order multi-symplectic RKN method and give some numerical comparisons with a 4-order non multi-symplectic RKN methods to illustrate the theoretical results in the previous sections.

We consider the following problem

$$\begin{aligned} &\mathrm{i}\psi_t + \alpha(t)\psi_{xx} + \theta(t)|\psi|^2\psi = 0,\\ &\psi(x,0) = \varphi(x), \end{aligned} \tag{4.1}$$

where

$$\alpha(t) = \frac{1}{2}\left(\cos(t) + \sqrt{2}\cos\left(\sqrt{2}t\right)\right), \quad \theta(t) = \frac{\cos(t) + \sqrt{2}\cos\left(\sqrt{2}t\right)}{\sin(t) + \sin\left(\sqrt{2}t\right) + 5},$$
$$\varphi(x) = \frac{1}{\sqrt{5}}\operatorname{sech}\left(\frac{x}{5}\right)\exp\left(\frac{\mathrm{i}(x^2-1)}{10}\right).$$

The equation is of interesting and important class (see [21] and references therein). Based on the results in [7,9,21], the problem has a quasi-periodically solitary wave solution

$$\psi_{qp}(x,t) = P_{1qp}(x,t)P_{2qp}(x,t)P_{3qp}(x,t), \tag{4.2}$$

where

$$P_{1qp}(x,t) = \frac{1}{(\sin(t) + \sin\left(\sqrt{2}t\right) + 5)^{\frac{1}{2}}},$$
$$P_{2qp}(x,t) = \operatorname{sech}\left(\frac{x}{\sin(t) + \sin\left(\sqrt{2}t\right) + 5}\right),$$
$$P_{3qp}(x,t) = \exp\left(\frac{\mathrm{i}(x^2-1)}{2\left(\sin(t) + \sin\left(\sqrt{2}t\right) + 5\right)}\right).$$

Since local and global momentum and charge are preserved, we define the errors of MCL and CCL by

$$(M_{\mathrm{err}})_l^n = (M_{le})_l^n/(h\tau) = \sum_{m=1}^{s} b_m \frac{(I(z_{l,m}^{n+1}) - I(z_{l,m}^{n}))}{\tau} + \sum_{k=1}^{r} \tilde{b}_k \frac{(G(z_{l+1}^{n,k}) - G(z_l^{n,k}))}{h} \tag{4.3}$$

and

$$(C_{\mathrm{err}})_l^n = (C_{le})_l^n/(h\tau) = \sum_{m=1}^{s} b_m \frac{(C(z_{l,m}^{n+1}) - C(z_{l,m}^{n}))}{\tau} + \sum_{k=1}^{r} \tilde{b}_k \frac{(J(z_{l+1}^{n,k}) - J(z_l^{n,k}))}{h} \tag{4.4}$$

respectively. $(M_{\mathrm{err}})_l^n$ and $(C_{\mathrm{err}})_l^n$ reflect the local numerical properties with solving the NLSE by using RKN discretizations (2.10), the indices l and n do not mean that the local errors are taken at the mesh point (x_l,t_n), for the reason that these errors are derived from the local integrations M_{le} and C_{le} in the rectangle

$$((x_l,t_n),(x_{l+1},t_n),(x_{l+1},t_{n+1}),(x_l,t_{n+1})).$$

From the approximations (4.3) and (4.4), we know that there exists an appropriate point, which is denoted by (x_l^*,t_n^*) in the rectangle and the errors are taken at this point.

As for the two global conserved quantities, the charge and total momentum, the global errors of them are defined as

$$\mathcal{C}_{\mathrm{err}}(n) = \mathcal{C}_d(n) - \mathcal{C}_d(0) \tag{4.5}$$

and

$$\mathcal{M}_{\mathrm{err}}(n) = \mathcal{M}_d(n) - \mathcal{M}_d(0) \tag{4.6}$$

respectively.

It is known that for the NLSEvc considered, the local and total energy are not conserved. To observe the evolution of the energy, notice that the exact local energy variation is given by

$$\begin{aligned} E_{\mathrm{ex}} \triangleq \partial_t E(z) + \partial_x F(z) &= \partial_t\left(-\frac{\theta(t)}{4}|\psi|^4 - \frac{\alpha(t)}{2}\Re(\overline{\psi}\psi_{xx})\right) + \partial_x\left(\frac{\alpha(t)}{2}\Re(\overline{\psi}\psi_{xt} - \overline{\psi_x}\psi_t)\right) \\ &= -\frac{\theta'(t)}{4}|\psi|^4 - \beta(t)|\psi|^2\Re(\overline{\psi}\psi_t) - \frac{\alpha'(t)}{2}\Re(\overline{\psi}\psi_{xx}) - \frac{\alpha(t)}{2}\Re(\overline{\psi_t}\psi_{xx} + \overline{\psi}\psi_{xxt}) \\ &\quad + \frac{\alpha(t)}{2}\Re(\overline{\psi}\psi_{xxt} - \overline{\psi_{xx}}\psi_t) \end{aligned} \tag{4.7}$$

and we make use of the notation $(E_{\mathrm{ex}})_l^n = E_{\mathrm{ex}}(\psi(x_l^*,t_n^*))$, and define the error of the local energy variation by

$$(E_{\mathrm{err}})_l^n = (E_{\mathrm{ex}})_l^n - (E_{le})_l^n/(h\tau), \tag{4.8}$$

where

$$(E_{le})_l^n/(h\tau) = \sum_{m=1}^{s} b_m \frac{(E(z_{l,m}^{n+1}) - E(z_{l,m}^{n}))}{\tau} + \sum_{k=1}^{r} \tilde{b}_k \frac{(F(z_{l+1}^{n,k}) - F(z_l^{n,k}))}{h}.$$

If the total energy is conserved in the continuous case, then under numerical discretizations, the global error of this quantity at some time step is defined by the difference between the current discrete total energy and the initial one [11,19]. It means that the initial discrete total energy derived from the corresponding discretization is regarded as the reference quantity to investigate the evolution of the energy. In this context, however, the total energy is not conserved in the continuous case. Hence in the numerical experiments, the initial discrete total energy cannot be seen as the reference quantity here at all. Now we define another discrete total energy at t_n by

$$\mathcal{E}_{\mathrm{ex}}(n) = h\sum_{l=0}^{N-1}\sum_{m=1}^{s} b_m\left(-\frac{\alpha(t_n)}{2}\Re\left(\overline{\psi(x_l+c_mh,t_0+n\tau)}\partial_{xx}\psi(x_l+c_mh,t_0+n\tau)\right) - \frac{\theta(t_n)}{2}V(|\psi(x_l+c_mh,t_0+n\tau)|^2)\right), \tag{4.9}$$

which is obtained by replacing the numerical nodal data in (2.27) by the corresponding exact ones. The discrete energy in (4.9) is another approximation to the exact total energy $\mathcal{E}(z)(t)$ at t_n and the approximation error depends only on the truncation error of the discretization of the spatial integration. With the upper bound of the truncation error given in [12], the approximation error of the discrete total energy in (4.9) can be controlled by means of choosing small enough spatial stepsize h. To make a difference from the discrete total energy in (2.27), the discrete total energy defined here is referred to the "exact" total energy. Naturally, we define the global error of the discrete total energy by

$$\mathcal{E}_{\mathrm{err}}(n) = \mathcal{E}_{\mathrm{ex}}(n) - \mathcal{E}_d(n). \tag{4.10}$$

The above errors listed are all the preserving errors of local and global conservation laws, the error of solutions, an important numerical characteristic, should be investigated. Here, we use the infinite norm of differences between the numerical and exact solutions, namely the following maximum error

$$(\eta_{\mathrm{err}})_l^n = \max(|\Re(\psi(x_l,t_n) - \psi_l^n)|, |\Im(\psi(x_l,t_n) - \psi_l^n)|). \tag{4.11}$$

In the subsequent numerical exhibitions, we use the following notations of maximum errors

$$(M_{\mathrm{err}})^n = \max_l |(M_{\mathrm{err}})_l^n|, \tag{4.12}$$

$$(C_{\mathrm{err}})^n = \max_l |(C_{\mathrm{err}})_l^n|, \tag{4.13}$$

$$(E_{\mathrm{err}})^n = \max_l |(E_{\mathrm{err}})_l^n|, \tag{4.14}$$

$$(\eta_{\mathrm{err}})^n = \max_l |(\eta_{\mathrm{err}})_l^n|. \tag{4.15}$$

Since the exact solution $\psi(x,t)$ given in (4) is also exponentially small away from $x = 0$ for any fixing t, the periodic boundary condition

$$\psi|_{x=x_{\mathrm{L}}} = \psi|_{x=x_{\mathrm{R}}}, \tag{4.16}$$

are added to the problem (4.1), we take $x_{\mathrm{L}} = -60$ and $x_{\mathrm{R}} = 60$, the temporal interval [0,200]. The spatial stepsize and the temporal one are take as $h = 0.6$ and $\tau = 0.1$, respectively in the following numerical experiments.

We construct the symplectic and non-symplectic 3-stage 4-order Nyström schemes, which can be formulated as the following Butcher's tabulars

0	$-1/4$	$1/4$	0
$1/2$	$7/48$	$-1/48$	0
1	$1/6$	$1/3$	0
	$1/6$	$1/3$	0
	$1/6$	$2/3$	$1/6$

and

0	0	0	0
$1/2$	$17/96$	$-1/6$	$11/96$
1	$1/24$	$2/3$	$-5/24$
	$1/6$	$1/3$	0
	$1/6$	$2/3$	$1/6$

respectively. We denote the multi-symplectic RKN method, i.e., the 2-stage 4-order Gauss–Legendre collocation method

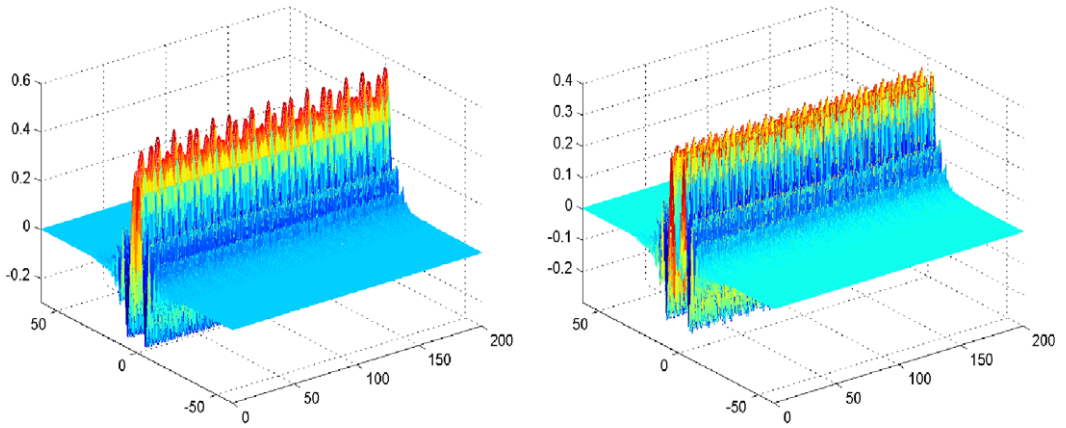

Fig. 1. The numerical quasi-periodically solitary solutions obtained by using MS-MN3, the real part $q(x,t)$ (left) and the imaginary part $p(x,t)$ (right).

$$\begin{array}{c|cc} \frac{1}{2}-\frac{\sqrt{3}}{6} & \frac{1}{4} & \frac{1}{4}-\frac{\sqrt{3}}{6} \\ \frac{1}{2}+\frac{\sqrt{3}}{6} & \frac{1}{4}+\frac{\sqrt{3}}{6} & \frac{1}{4} \\ \hline & \frac{1}{2} & \frac{1}{2} \end{array}$$

applied to the temporal and the above 3-stage 4-order symplectic Nyström scheme to the spatial direction, by MS-MN3 in short. And, the non-multisymplectic one is denoted by nMS-MN3, which is concatenation of the 2-stage 4-order Gauss–Legendre collocation method in the temporal direction and the above 3-stage 4-order non-symplectic Neström scheme in the spatial direction. All numerical comparisons between MS-MN3 and nMS-MN3 are processed under the same numerical conditions. Because two methods are implicit, the fixed point iteration method is utilized to solve the nonlinear algebraic systems generated by the numerical scheme, each iteration will terminate when the maximum absolute error of the adjacent two iterative values is less than 10^{-14}. The time cost of the scheme MS-MN3 is about 3/4 of that of the non-multisymplectic one, nMS-MN3. Figs. 1–8 are given by means of the two methods, MS-MN3 and nMS-MN3.

Fig. 1 shows the numerical solutions of the quasi-periodically solitary wave obtained by MS-MN3. It reflects some theoretical properties of the exact quasi-periodically solitary wave solution, e.g. the asymptotic behavior in the space and the quasi-periodicity in the time. The results of numerical simulation with nMS-MN3 are as good as ones with MS-MN3, we do not plot the two graphs obtained by the former any more accordingly.

The numerical results related to the local energy variation are listed in Fig. 2. The error obtained by Ms-MN3 is in the scale of $\mathcal{O}(10^{-2})$ and that by nMS-MN3 is only $\mathcal{O}(10^{-1})$. From the top two diagrams and bottom one, with the errors exhibited at the middle, one concludes that the multi-symplectic scheme MS-MN3, on simulating the local energy variation, is a little better than the non-multi-symplectic one, nMS-MN3.

Fig. 3 displays the numerical results of the total energy. The discrete total energy obtained by MS-MN3, the corresponding one obtained by nMS-MN3 and the exact total energy are almost the same in the present scale. As appearing in Fig. 2, the error obtained by MS-MN3 is a little better than that by nMS-MN3, the former is of order $\mathcal{O}(10^{-3})$ and the other is only of $\mathcal{O}(10^{-1})$. The two error curves evolves very similarly, they have some reasonable oscillations and do not produce any error accumulation over the time interval. The stability of the two high-order schemes with respect to the total energy is verified numerically.

Fig. 4 shows the maximum errors of the discrete momentum conservation law in the time interval [0,200]. From the two graphs, the preserving order, the oscillation, the evolution of errors obtained by

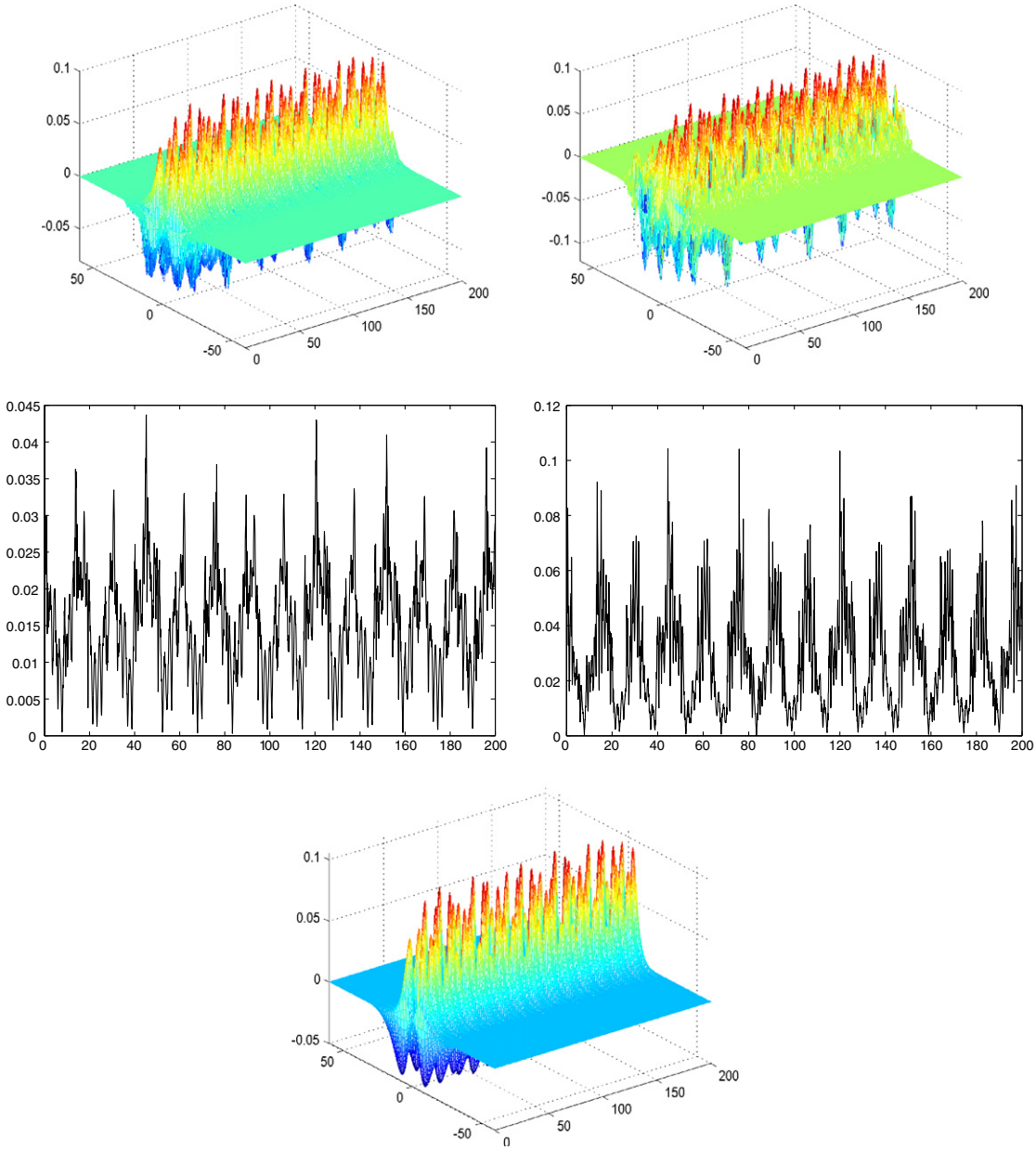

Fig. 2. The discrete local energy variation obtained by MS-MN3 (left-top) and nMS-MN3 (right-top); the middle is the maximum errors of the local energy variation, MS-MN3 (left-mid) and nMS-MN3 (right-mid); the bottom is the exact local energy variation.

MS-MN3 and nMS-MN3 are almost the same. It is further shown in Fig. 5 that the global errors in preserving the total momentum by the two schemes are very similarly. The error curves in the two figures show numerically that the two schemes are stable in the sense of the local and global momentum conservation laws (see [4]).

The maximum errors of the local charge conservation law by the two high-order schemes are exhibited in Fig. 6. The left graph shows that the local charge conservation law is preserved in the scale of $\mathcal{O}(10^{-15})$, almost roundoff errors of the computer by means of MS-MN3, however, the error obtained by nMS-MN3 is only of $\mathcal{O}(10^{-2})$. Similar numerical phenomena are exhibited in Fig. 7 on the global errors in preserving the discrete

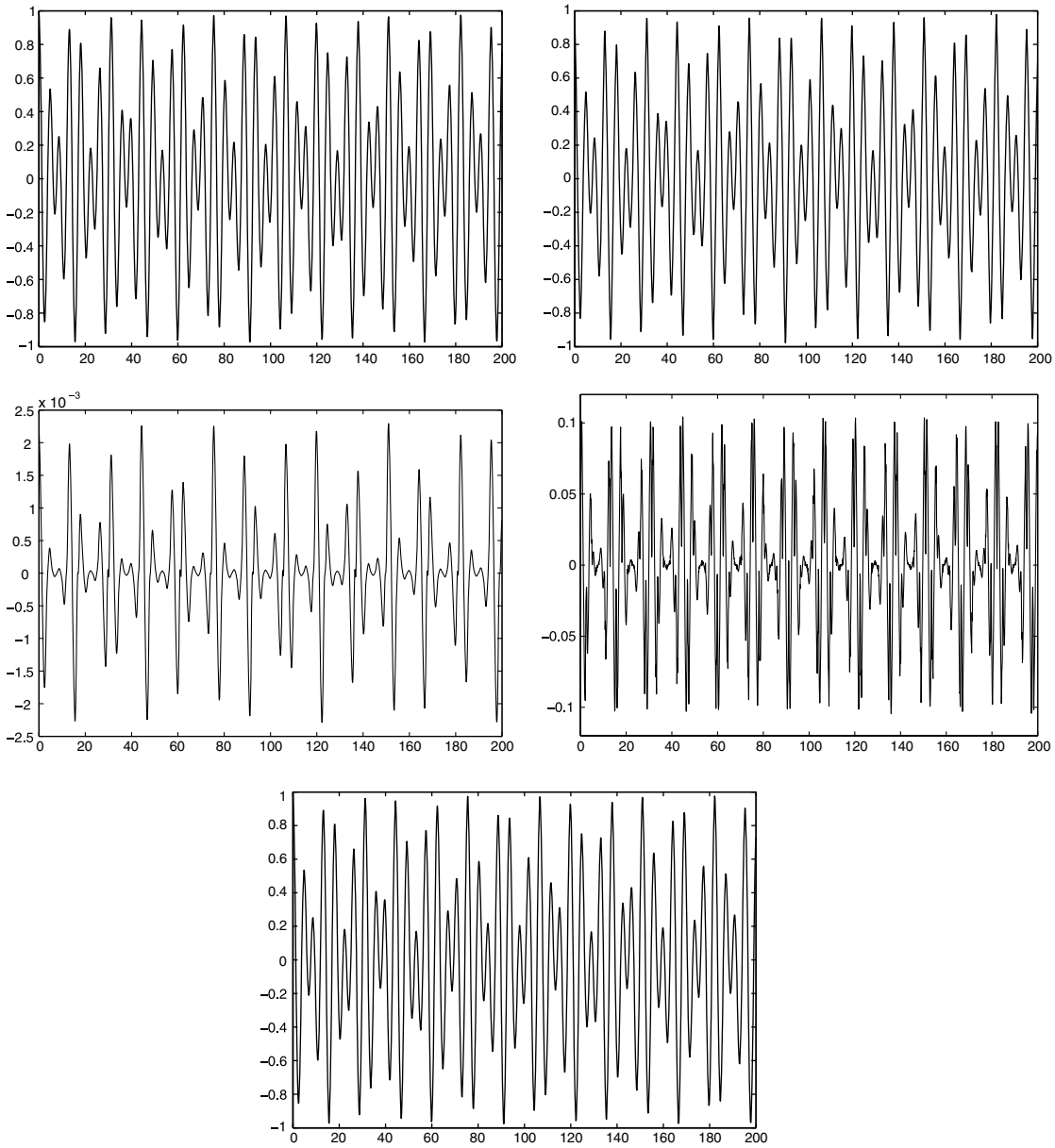

Fig. 3. Left-top: the discrete total energy obtained by MS-MN3; right-top: the discrete total energy obtained by MS-MN3; mid-left: the global error of the total energy by MS-MN3; mid-right: the global error of the total energy by nMS-MN3; bottom: the exact total energy.

charge. Comparing the four graphs in Figs. 6 and 7, we find that the remarkable advantages of multi-symplectic RKN methods are the precise preservations of the charge conservation laws.

Fig. 4 shows the maximum errors of the numerical solutions by MS-MN3 and nMS-MN3 in the time interval [0,200], and reveals that the errors are almost the same. The peak value of the errors by MS-MN3 is about 0.1 and that by nMS-MN3 is about 0.16. The two error curves present almost the same reasonable oscillations.

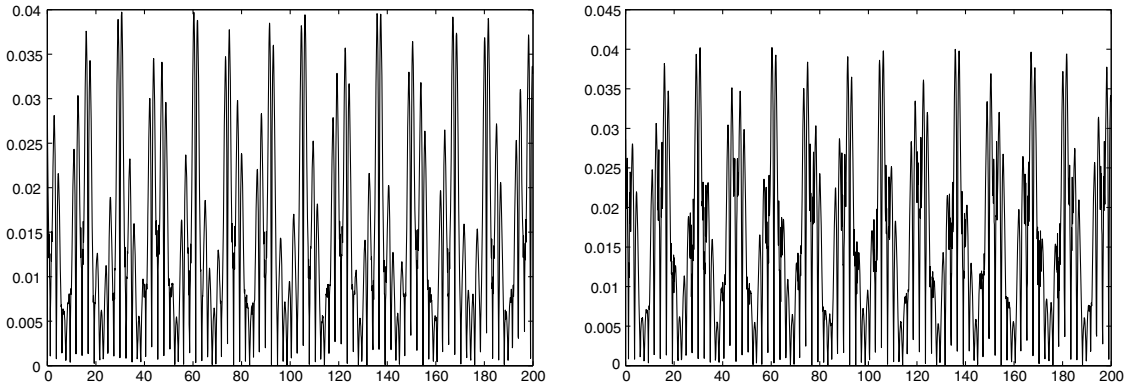

Fig. 4. The maximum errors of the discrete local momentum conservation law, MS-MN3 (left) and nMS-MN3 (right).

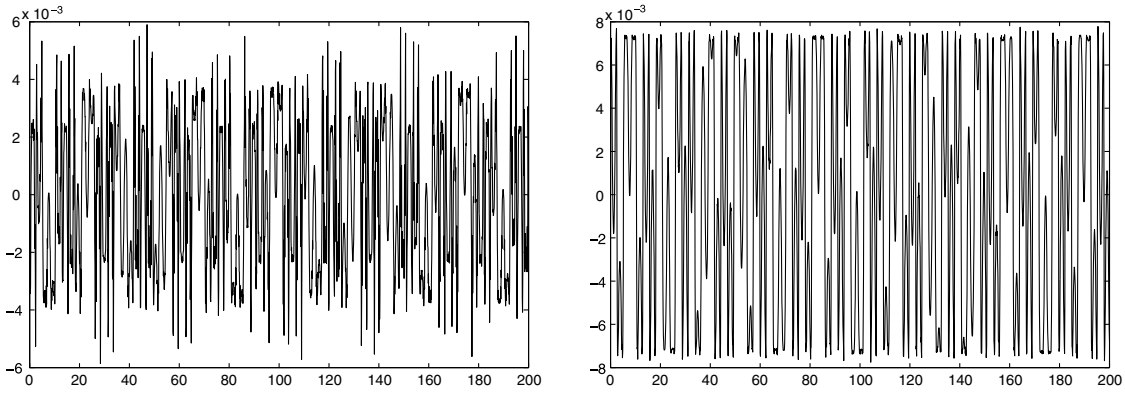

Fig. 5. The global errors of the discrete total momentum, MS-MN3 (left) and nMS-MN3 (right).

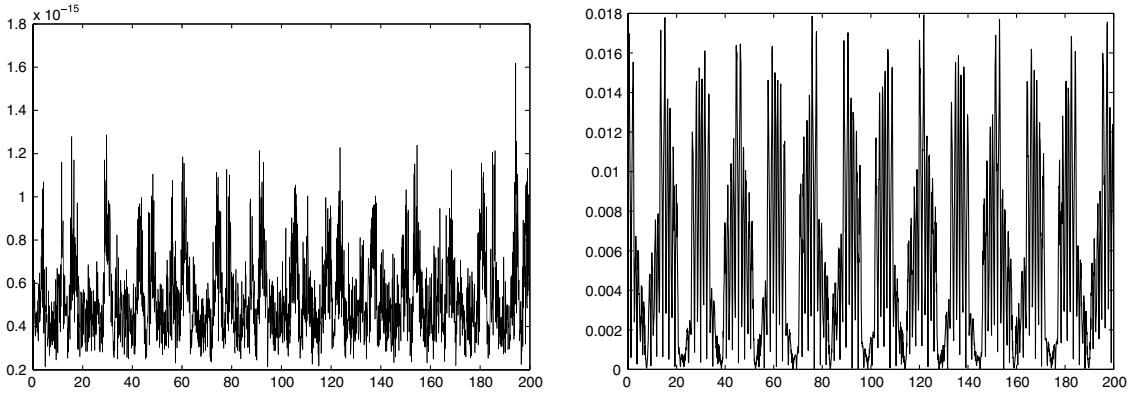

Fig. 6. The maximum errors of the discrete local charge conservation law, MS-MN3 (left) and nMS-MN3 (right).

5. Conclusions

The concatenation of symplectic Runge–Kutta methods in temporal direction and symplectic Nyström methods in spatial direction for NLSEvc leads to the multi-symplectic integrators. It is shown theoretically that the discrete total symplecticity in temporal direction is preserved precisely by the multi-symplectic

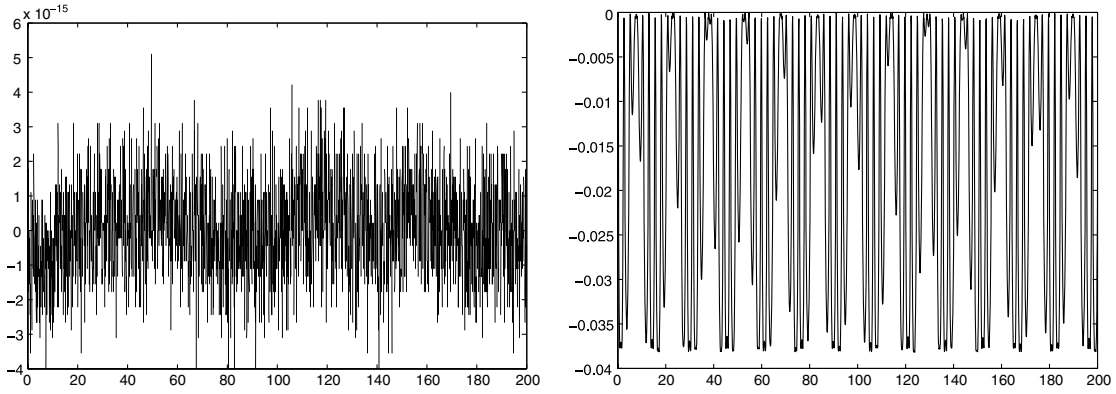

Fig. 7. The global errors of the discrete charge, MS-MN3 (left) and nMS-MN3 (right).

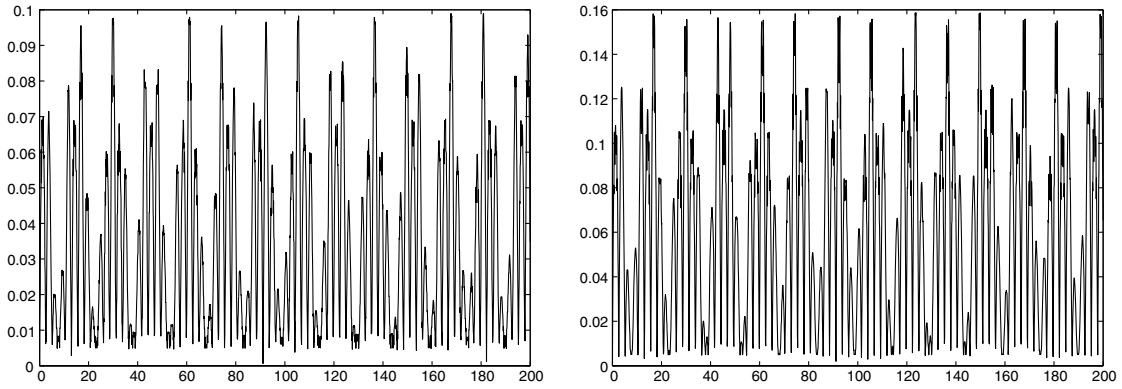

Fig. 8. The maximum errors of the numerical solutions, MS-MN3 (left) and nMS-MN3 (right).

RKN methods for NLSEvc. Numerical results reveal the stability of multi-symplectic RKN methods in the sense of classical conservation laws and the good preservation of phase space structure. Theoretical and numerical results show that the remarkable advantage of multi-symplectic RKN methods is the precise preservation of discrete (local and global) charge conservation law for NLSEvc. An interesting observation is that the numerical accuracy of total energy under the multi-symplectic RKN discretization may reach in a higher order in contrast to the accuracy of numerical schemes. A 4-order multi-symplectic RKN scheme is presented and implemented in numerical experiments. Some interesting numerical results reveal the superiorities of multi-symplectic RKN methods not only in the conservation of multi-symplectic geometric structure, but also in the preservation of some crucial conservative properties in physics.

Acknowledgement

The authors are grateful to the referees for their helpful comments and important suggestions.

References

[1] U.M. Ascher, R.I. McLachlan, On symplectic and multisymplectic schemes for the KdV equation, J. Sci. Comput. 25 (2005) 83–104.
[2] T.J. Bridges, Muti-symplectic structures and wave propagation, Math. Proc. Camb. Phil. Soc. 121 (1997) 147–190.
[3] T.J. Bridges, S. Reich, Multi-symplectic integrators: numerical schemes for Hamiltonian PDEs that conserve sysmplecticity, Phys. Lett. A 284 (2001) 184–193.
[4] B. Cano, Conserved quantities of some Hamiltonian wave equations after full discretization, Numer. Math. 103 (2006) 197–223.
[5] Q. Chang, E. Jia, W. Sun, Difference schemes for solving the generalized nonlinear Schrödinger equation, J. Comput. Phys. 148 (1999) 397–415.

[6] E. Hairer, C. Lubich, G. Wanner, Geometric Numerical Integration, Springer-Verlag, Berlin, Heidelberg, 2002.
[7] J. Hong, Y. Liu, A novel numerical approach to simulating nonlinear Schrödinger equation with varying coefficients, Appl. Math. Lett. 16 (2003) 759–765.
[8] J. Hong, Y. Liu, Multi-symplecticity of the centred box discretization for a class of Hamiltonian PDEs and an application to quasi-periodically solitary wave of $qpKdV$ equation, Math. Comput. Model. 39 (2004) 1035–1047.
[9] J. Hong, Y. Liu, Hans Munthe-Kaas, Antonella Zanna, Globally conservative properties and error estimation of a multi-symplectic scheme for Schrödinger equations with variable coefficients, Appl. Numer. Math. 56 (2006) 814–843.
[10] J. Hong, H. Liu, G. Sun, The Multi-symplecticity of partitioned Runge–Kutta methods for Hamiltonian PDEs, Math. Comput. 75 (2006) 167–181.
[11] J. Hong, C. Li, Multi-symplectic Runge–Kutta methods for nonlinear Dirac equations, J. Comput. Phys. 211 (2006) 448–472.
[12] A. Iserles, A First Course in the Numerical Analysis of Differential Equations, Cambridge University Press, Cambridge, 1996.
[13] A.L. Islas, D.A. Karpeev, C.M. Schober, Geometric integrators for the nonlinear Schrödinger equation, J. Comput. Phys. 173 (2001) 116–148.
[14] A.L. Islas, C.M. Schober, On the preservation of phase space structure under multisymplectic discretization, J. Comput. Phys. 197 (2004) 585–609.
[15] B. Leimkuhler, S. Reich, Simulating Hamiltonian Dynamics, Cambridge Monographs on Applied and Computational Mathematics 14, Cambridge University Press, Cambredge, 2004.
[16] J.E. Marsden, S. Pekarsky, S. Shkoller, M. West, Variational methods, multisymplectic geometry and continuum mechanics, J. Geom. Phys. 38 (2001) 253–284.
[17] B. Moore, S. Reich, Multisymplectic integration methods for Hamiltonian PDEs, Future Gener. Comput. Syst. 19 (2003) 395–402.
[18] B. Moore, S. Reich, Backward error analysis for multi-symplectic integration methods, Numer. Math. 95 (2003) 625–652.
[19] S. Reich, Multi-symplectic Runge–Kutta collocation methods for Hamiltonian wave equation, J. Comput. Phys. 157 (2000) 473–499.
[20] J.M. Sanz-Serna, M.P. Calvo, Numerical Hamiltonian Problems, Chapman & Hall, London, 1994.
[21] V.N. Serkin, A. Hasegawa, Novel soliton solutions of the nonlinear Schrödinger equation model, Phys. Rev. Lett. 85 (2000) 4502–4505.
[22] Y.B. Suris, On the conservation of the symplectic structure in the numerical solution of Hamiltonian systems (in Russian), in: S.S. Filippov (Ed.), Numerical Solution of Ordinary Differential Equations, Keldysh Institute of Applied Mathematics, USSR Academy of Sciences, Moscow, 1988, pp. 148–160.
[23] Y.B. Suris, The canonicity of mapping generated by Runge–Kutta type methods when integrating the systems $\ddot{x} = -\partial U/\partial x$, Zh. Vychisl. Mat. i Mat. Fiz. 29 (1989) 138–144.